Synthesis, structural and physicochemical characterization of a new type Ti_6-oxo cluster protected by a cyclic imide dioxime ligand

Stamatis S. Passadis,[a] Sofia Hadjithoma,[b] Angelos G. Kalampounias,[c] Athanassios C. Tsipis,[*a] Stephen Sproules,[*d] Haralampos N. Miras,[*d] Anastasios D. Keramidas[*b] and Themistoklis A. Kabanos[*a]

*Corresponding authors

[a]Section of Inorganic and Analytical Chemistry, University of Ioannina, Ioannina 45110, Greece
E-mail: tkampano@cc.uoi.grand, attsipis@uoi.gr

[b]Department of Chemistry, University of Cyprus, Nicosia 2109, Cyprus
E-mail: akeramid@ucy.ac.cy

[c]Physical Chemistry, Department of Chemistry, University of Ioannina, Ioannina 45110, Greece

[d]West CHEM, School of Chemistry, University of Glasgow, Glasgow G12 8QQ, UK
E-mail: stephen.sproules@glasgow.ac.uk, harism@chem.gla.ac.uk

Abstract

Reaction of the cyclic ligand (2*Z*,6*Z*)-piperidine-2,6-dione dioxime with $TiCl_4$ and KOH yielded the hexanuclear cluster $K_6[Ti^{IV}_6(\mu_3\text{-}O)_2(\mu_2\text{-}O)_3(CH_3O)_6(\mu_2\text{–}\eta^1,\eta^1,\eta^2\text{-Hpidiox-}O,N,O')_4(\mu_2\text{–}\eta^1,\eta^1,\eta^2\text{-pidiox-}O,N,O')_2]\cdot 7.5CH_3OH$ possessing a new $\{Ti_6O_5\}$ structural motif. The cluster core $\{Ti_6O_5\}$ is wrapped by external tripodal imide dioxime ligands, showing good solubility and stability and thus, allowing its solution to be studied by means of electrospray ionization mass spectrometry, electrochemistry and 2D NMR, c. w. EPR and UV-vis spectroscopies. Density Functional Theory (DFT) calculations reveal that the *cyclo*-Ti_3 metallic cores exhibit metallaromaticity which is expected to contribute to the stabilization of this system.

Introduction

Crystalline polyoxo-titanium clusters (PTCs) have attracted considerable attention the last years[1–12] due to their potential applications in catalysis, medicine, electro-optics, and nanotechnology.[13–19] In particular, the precise structural information of PTCs can help the understanding of the binding modes of sensitizers to Ti–O[20]surfaces and potential applications in photoelectronic[21–24] and photocatalytic chemistry.[2,25–29] Moreover, the development of more efficient TOC photocatalysts for waste water treatment and splitting of the water is a hot topic in renewable energy and environmental research.

Organic chelators could enhance the photocatalytic activity of PTCs and protect the Ti–O cores from hydrolysis.[27,30] The ligand (2*Z*,6*Z*)-piperidine-2,6-dione dioxime (H_3pidiox, Scheme 1) which stabilizes hard metals in their high oxidation states and protects them from hydrolysis was chosen as a chelator.

The ligand H_3pidiox in its mono/di and tri-deprotonated form acts as a tridentate chelator in its metal complexes with U^{VI}, $\{[U^{VI}O_2(Hpidiox)_2]\}$,[31] Fe^{III}, $\{[Fe^{III}(Hpidiox)(H_2pidiox)]\}$[32] and $V^{IV/V}$, $\{[V^{IV/V}(pidiox)_2]^{2-/-}\}$.[33,34] The hydrolytic stability of the ligand H_3pidiox was reported by Hay and co-workers.[35]

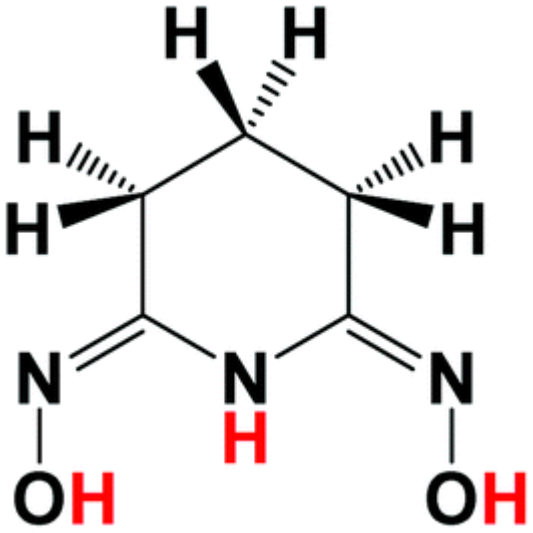

Scheme 1 The ligand H_3pidiox.

In this study, it is described the synthesis and physicochemical characterization of a new hexanuclear $\{Ti_6O_5\}$ PTC, of which the *cyclo*-Ti_3 metallic cores exhibit metallaromaticity. The hexanuclear cluster **1** is soluble in CH_3OH and H_2O and in both solvents retains its structural integrity.

Experimental section

Synthesis of the organic molecule (2*Z*,6*Z*)-piperidine-2,6-dione dioxime (H_3pidiox)

Pentanedinitrile (4.700 g, 49.93 mmol) and hydroxylamine (50% in water) (7.250 g, 109.7 mmol) were added to a solution of C_2H_5OH/H_2O (100 mL, 1 : 1 v/v). The solution was refluxed at 86 °C (oil bath temperature 100 °C) under magnetic stirring for five days. Then, the solution was cooled to room temperature (25 °C) and the white precipitate was filtered and washed (2 × 10 mL) with cold ethyl alcohol (0 °C) and dried in vacuum to get 5.000 g of H_3pidiox. Yield, 70% (based on pentanedinitrile). The white solid was recrystallized with ethyl alcohol (1.000 g per 50 mL of C_2H_5OH) to get 2.150 g (yield of recrystallization 43%) of pure sample. Melting point: 190 °C (decomposes). Elemental anal. calc. for ($C_5H_9N_3O_2$, M_r = 143.15 g mol^{-1}): C 41.95, H 6.34, N 29.35; found: C 41.92, H 6.32, N 29.28.

Synthesis of $K_6[Ti^{IV}_6(\mu_3\text{-}O)_2(\mu_2\text{-}O)_3(CH_3O)_6(\mu_2\text{–}\eta^1,\eta^1,\eta^2\text{-}Hpidiox\text{-}O,N,O')_4(\mu_2\text{–}\eta^1,\eta^1,\eta^2\text{-}pidiox\text{-}O,N,O')_2]\cdot 7.5CH_3OH$ (1)

To a stirred moist methyl alcohol solution (2 ml) were successively added H_3pidiox (160 mg, 1.11 mmol), and $Ti^{IV}Cl_4$ (0.061 ml, 0.105 g, 0.555 mmol). The color of the solution turned red. Then, upon addition of solid KOH (62.7 mg, 1.11 mmol) in one portion an orange precipitate was formed which

was filtered off and the red filtrate was kept at ≈4 °C for two days during which period of time orange crystals of the hexanuclear titanium compound were formed. The crystals were filtered to obtain 98.6 mg of compound **1** (56%, based on $TiCl_4$). Elemental anal. calc. for ($C_{36}H_{60}N_{18}O_{23}K_6Ti_6 \cdot 7.5CH_3OH$, M_r = 1873.07 g mol^{-1}): C 27.89, H 4.74, N 13.46; found: C 27.72, H 4.57, N 13.28.

Results and discussion

Crystal structure

Ball-and-stick representations of the structure of the anion of **1**, along with the polyhedral/ball-and-stick view of the metallic core are shown in Fig. 1. The centrosymmetric structure of the **$^{IV}_{63}$-O)$_2$(μ_2-O)$_3$(CH_3O)$_6$(μ_2–η^1,η^1,η^2-Hpidiox-*O*,*N*,*O*′)$_4$(μ_2–η^1,η^1,η^2-pidiox-*O*,*N*,*O*′)$_2$]$^{6-}$** anion consists of two almost planar [Ti_3-μ_3-O] moieties in the eclipsed conformation (Fig. 1A) which are bridged by three μ_2-O^{2-} ligands, thus leading to the formation of the **[Ti_6O_5]** oxo-core. Each of the six doubly and triply deprotonated ligands, Hpidiox^{2-}/pidiox^{3-}, which decorate the two [Ti_3-μ_3-O] structural units, acts as a μ_2-bridging ligand through its oxime oxygen atom, while the hydroxylamine and oxime oxygens and the imine nitrogen atoms form two five-membered chelate rings (Scheme 2) with each titanium atom. All the titanium atoms adopt a distorted NO_6 pentagonal bipyramidal coordination environment and are bonded to a μ_3-O^{2-} [O(3)] and a μ_2-O^{2-} [O(4)] bridges, two μ_2-bridging oxime oxygens [O(2)–O(2)′], a hydroxylamine oxygen [O(1)] atom, a methoxy oxygen [O(5)] atom and an imine nitrogen [N(2)] atom (Fig. 1C).

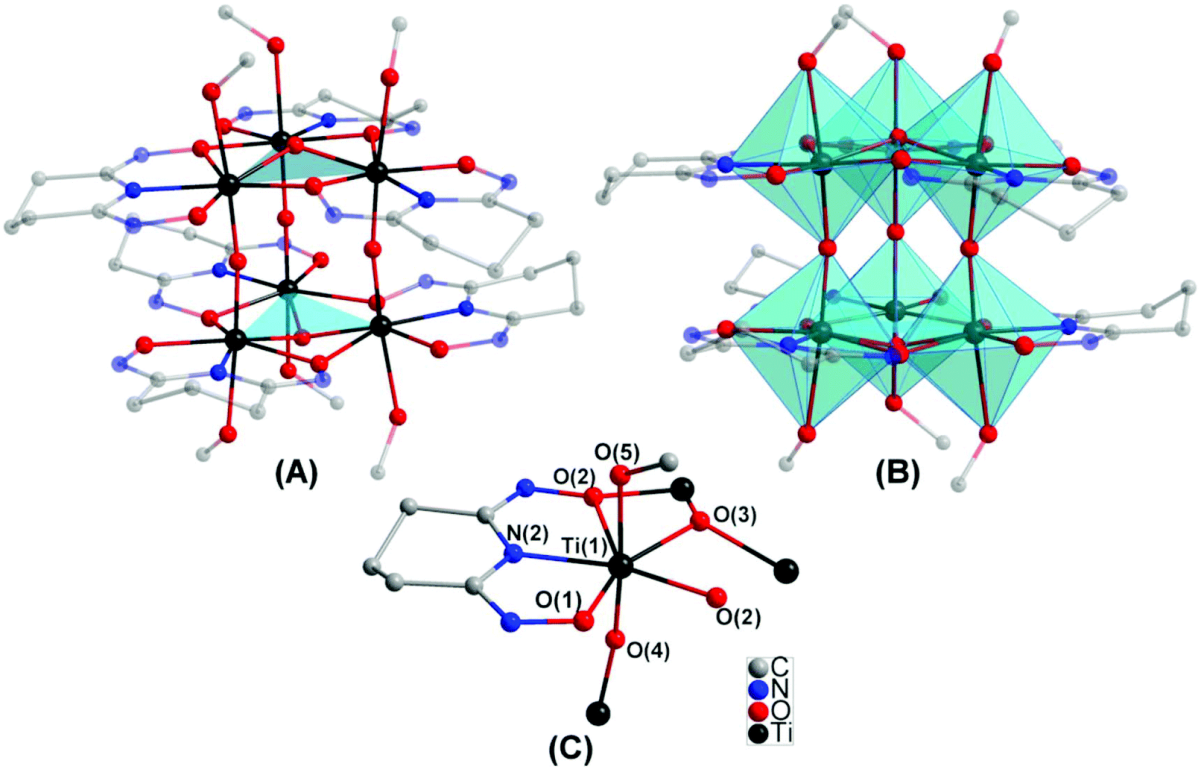

*Figure 1 Ball-and-stick representations of the anion of the hexanuclear titanium cluster (A), the polyhedral/ball-and-stick view of the anion of **1** (B) and the coordination environment of the titanium atoms (C).*

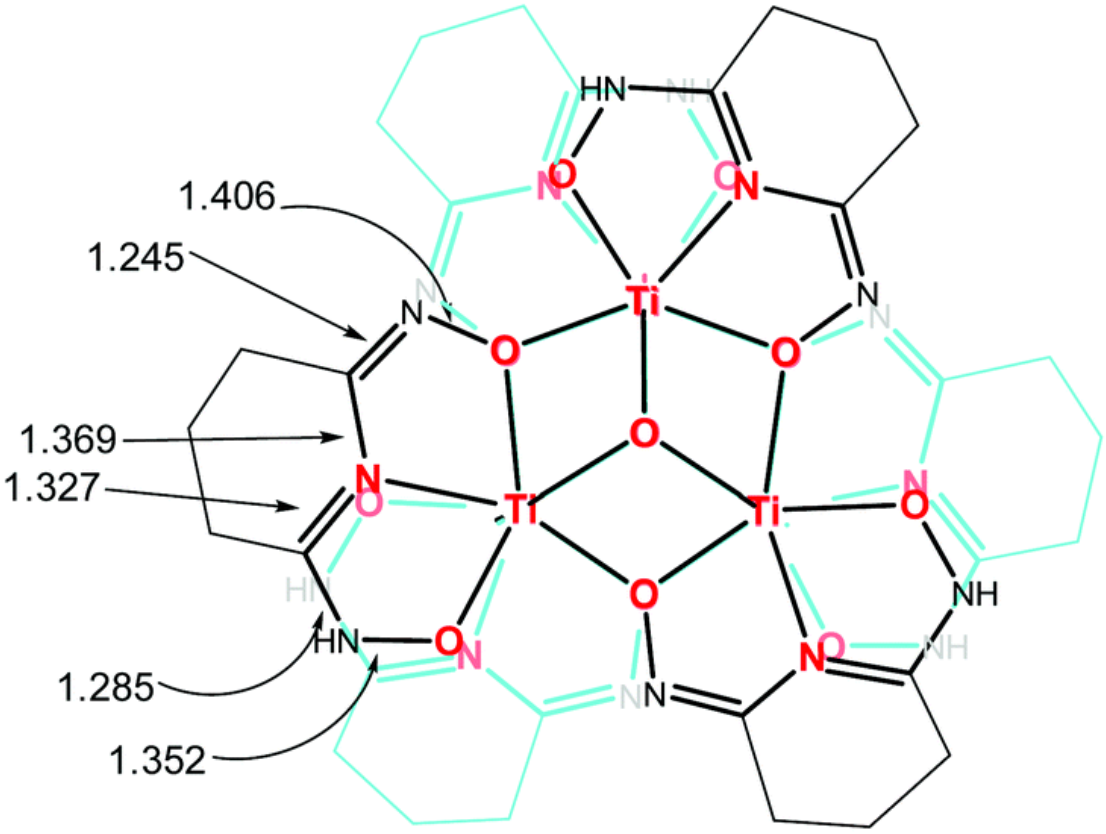

*Scheme 2 A sketch of the structure of the anion of **1** viewed along the c axis showing the arrangement of the ligands.*

The bond distances of Ti–μ_2-O^{2-} [1.795(1) Å] and Ti–μ_3-O^{2-} [1.931(2) Å] are in the expected range.[3,7,9–11,22,25,36–56] The *d*(Ti–$O_{hydroxylamine}$) = 2.002(6) Å is shorter than the *d*(Ti–O_{oxime}) = 2.088(5) Å reflecting the better donor properties of $O_{hydroxylamine}$ in comparison with the O_{oxime} atoms (Scheme 2). The *d*(Ti–O_{oxime}) in **1** is larger than the Ti–O_{oxime} distances of other Ti^{IV}-oximates reported in the literature, which is due to the different coordination mode, end-on in **1***vs*. side on in those in literature.[57,58] The strong *trans* effect of μ_2-O^{2-}ligand results in the elongation of the Ti–$O_{methoxy}$ bonds [2.179(2) Å]. The two symmetry related μ_3-O^{2-} atoms in the two [Ti_3-μ_3-O] structural units are located 0.489 (5) Å above the plane defined by the three titanium atoms. The long-short pattern of the bond lengths of O(1)–N(1)–C(1)–N(2)–C(5)–N(3)–O(2) (1.352, 1.285, 1.327, 1.369, 1.245, 1.406 Å respectively) supports the suggested hydroxylamine-oxime form for the ligand (Scheme 2). A similar pattern of the bond lengths of the ligand $Hpidiox^{2-}$/$H_2pidiox^-$ has been observed in the iron(iii) complex [Fe^{III}(Hpidiox)(H_2pidiox)].[32] In the interior of the {Ti_6O_5} cluster there is a void space with dimensions 4.11 × 4.52 Å. To the best of our knowledge, though the **{Ti_6O_5}** core has been reported only once,[37] its topology in compound **1**(Fig. 2A) is quite different in comparison with the previously reported one (Fig. 2B). The main differences between them are: (i) the coordination number of the six titanium atoms is seven in comparison to six, and (ii) the six titanium atoms are in an almost ideal trigonal prismatic arrangement (Fig. 2C), while in the reported **{Ti_6O_5}** core of [Ti_6O_5(O^iBu)$_6$(OOC^iBu)$_8$] the six titanium atoms are in an almost co-planar configuration (Fig. 2B).[37]

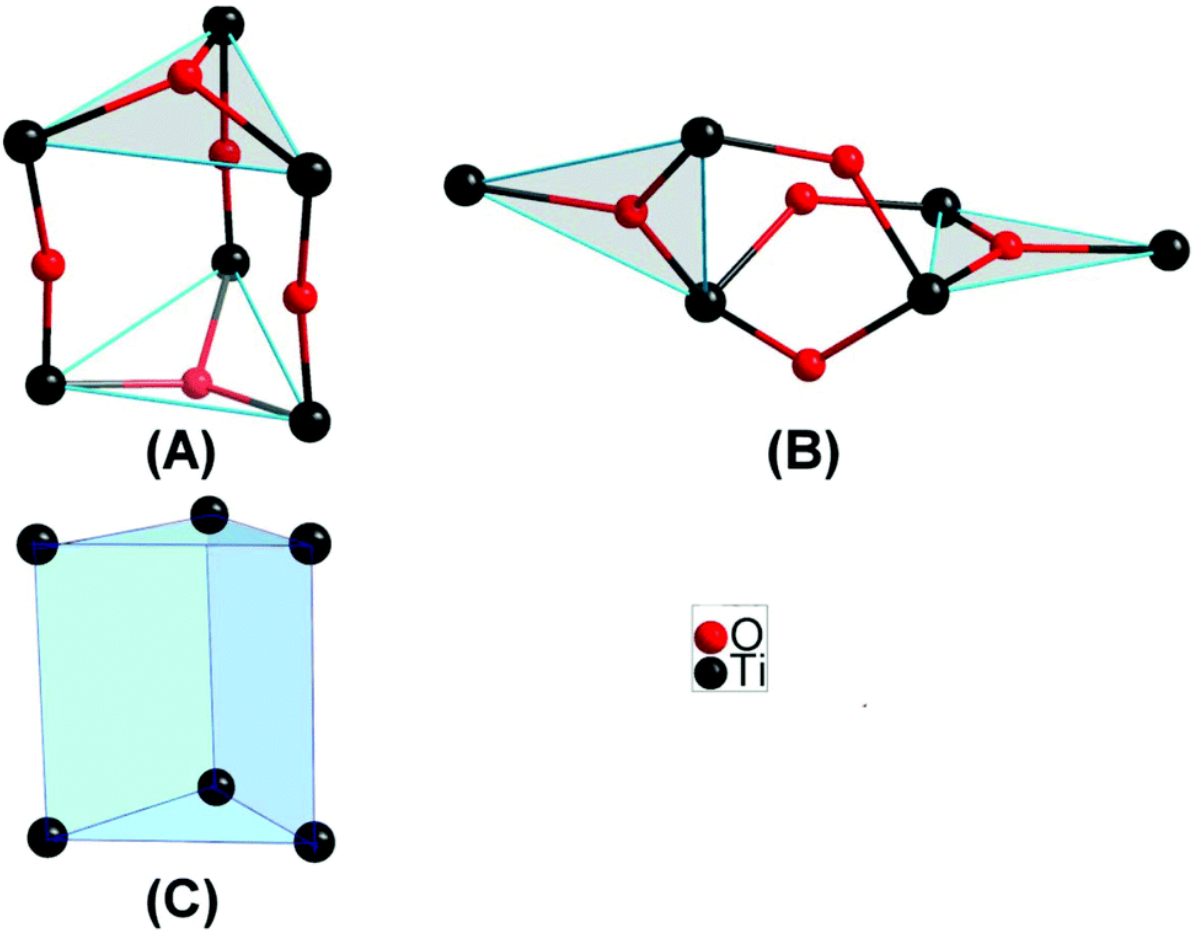

Figure 2 - The structures of the ***[Ti$_6$O$_5$]*** *core in compound* ***1*** *(A) and [Ti$_6$O$_5$(O^{i}Bu)$_6$(OOC^{i}Bu)$_8$][37] (B) and the arrangement of the six titanium atoms in* ***1*** *(C).*

At this point, it is worth noting that eight different types of titanium-polyoxo hexamers have been reported (Fig. 3a–k). As shown in Fig. 3, the basic skeletal arrangements of Ti_6 oxo-clusters are: (i) two $\{Ti_6(\mu_3\text{-}O)_6\}$ configurations, one with a ball like structure (Fig. 3a),[36,37] and the second one consisting of two planar $\{Ti_3O_3\}$ units parallel to each other (Fig. 3b);[12,27–39,42] (ii) six configurations with the six Ti^{IV} lying almost on a planar arrangement $\{Ti_6(\mu_2\text{-}O)_9\}$ (Fig. 3c),[51] $\{Ti_6(\mu_2\text{-}O)_2(\mu_4\text{-}O)_2\}$ (Fig. 3d),[44] $\{Ti_6(\mu_3\text{-}O)_4\}$ (Fig. 3g),[22,47,50] $\{Ti_6(\mu_3\text{-}O)_2(\mu_2\text{-}O)\}$ (Fig. 3h),[40,42]$\{Ti_6(\mu_3\text{-}O)_2(\mu_2\text{-}O)_2\}$ (Fig. 3i),[16] $\{Ti_6(\mu_3\text{-}O)_2(\mu_2\text{-}O)_3\}$ (Fig. 3j),[27] (iii) two configurations, $\{Ti_6(\mu_2\text{-}O)_8\}$ (Fig. 3e)[55] and $\{Ti_6(\mu_2\text{-}O)_9\}$ (Fig. 3f),[56] exhibiting two $\{Ti_3(\mu_2\text{-}O)_3\}$ units parallel to each other; and (iv) $\{Ti_6(\mu_3\text{-}O)_2(\mu_2\text{-}O)_2\}$ (Fig. 3k),[15,43–48] exhibiting two $\{Ti_3(\mu_3\text{-}O)\}$ units parallel to each other.

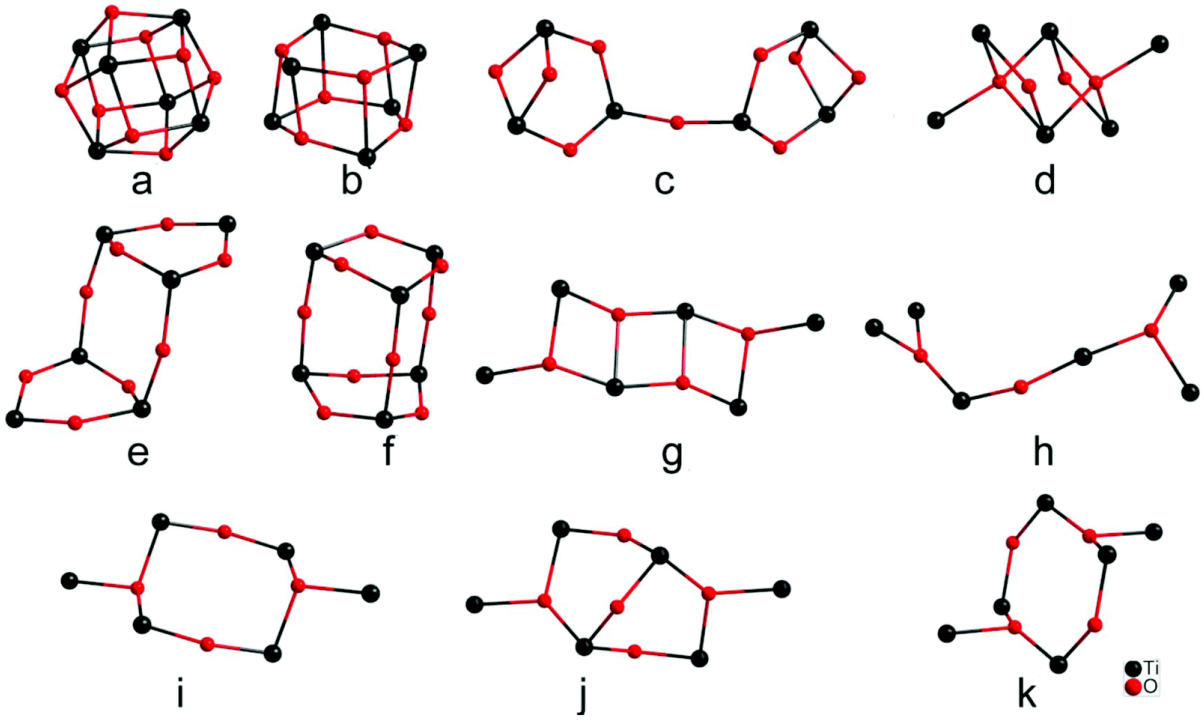

Figure 3 - Skeletal arrangements of the Ti_6 oxo-metallic cores (only the titanium and bridging oxygen atoms are shown for clarity).

CW EPR spectroscopic study

The CW EPR spectrum of **1** in methanol gave no signal in either room temperature or liquid helium and this implies that the oxidation state of the six titanium atoms in **1** is IV.

FT-IR spectroscopic study

Fig. 4 shows the FT-IR spectra obtained for the complex **1** in the solid state at ambient conditions, along with the corresponding spectrum of the ligand H_3pidiox for comparison. The high-frequency region of the spectra is dominated by the presence of the N–H, OH and C–H stretching modes and does not provide insight into the structural features of the titanium complex. Thus, we focus our attention to the high-frequency region, namely the fingerprint region which is dominated by a large number of strongly overlapping bands designating the structural complexity of the system under study. Several bands emerge in the FT-IR spectrum that are absent in the spectrum of ligand and can be attributed to titanium complex formation. The intense bands located at 854 and 788 cm^{-1} are assigned to the high energy *ν*(Ti–O) stretching modes. Furthermore, two bands appear near ~1598 and ~492 cm^{-1} with medium absorbance, while two additional weak bands are also shown in the spectra around ~625 and ~426 cm^{-1}. The spectroscopic data further justify the structure proposed by other experimental techniques used in this study.

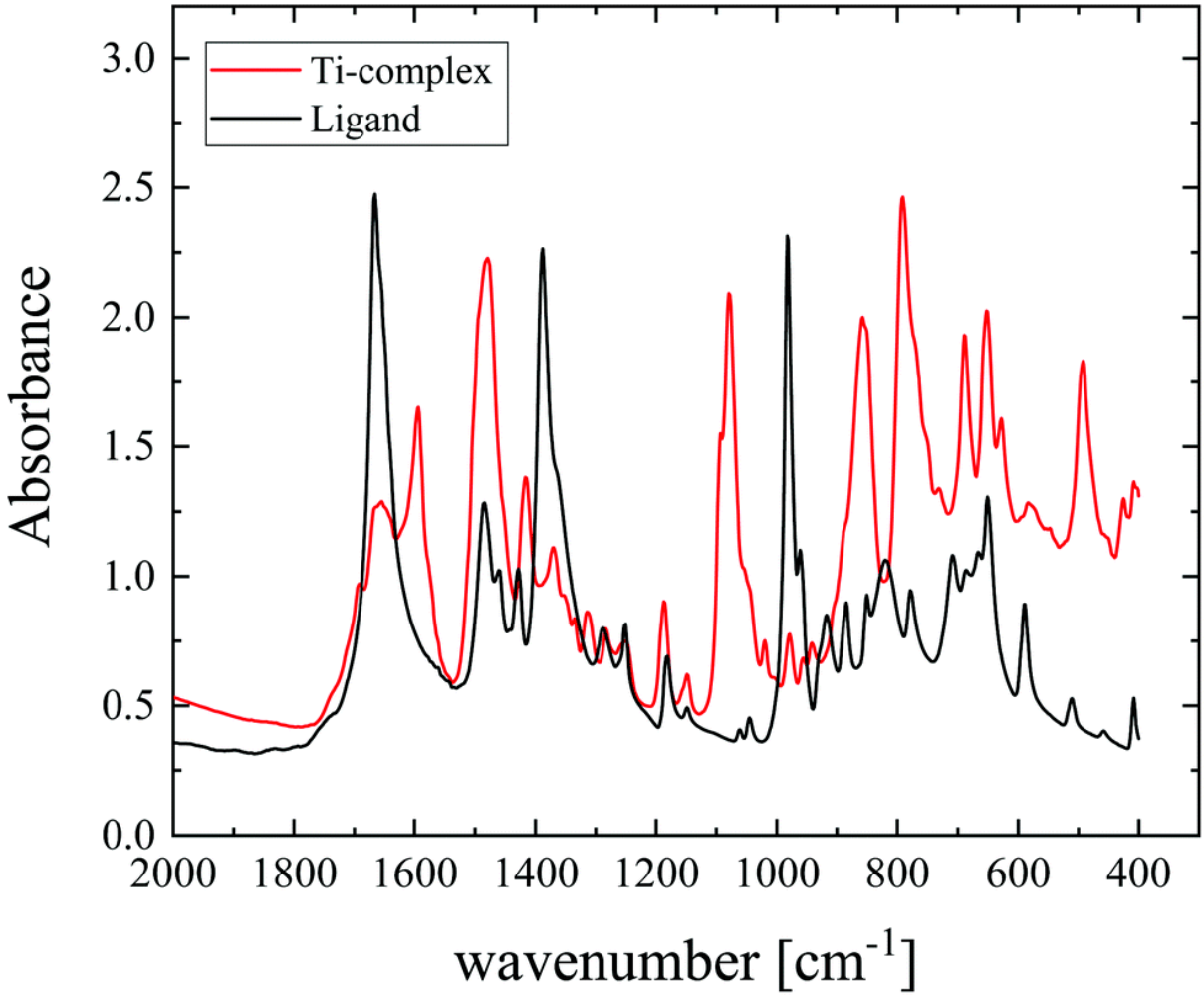

Figure 4 - Fingerprint region of the FTIR spectra of the ligand H3pidiox (black line) and titanium complex 1 (red line) at ambient conditions.

Electrochemistry

The cyclic voltammogram (CV) of the ligand H_3pidiox in methanol solution gave an irreversible reduction peak at −410 mV. The CV of **1** in methyl alcohol solution gave a two-electron irreversible anodic peak at 1200 mV *vs.*NHE (Fig. 5), assigned to the oxidation of the two pidiox^{3-} ligands as predicted by the theory (*vide infra*). The oxidation potential of the ligand was presumably decreased upon its coordination to the titanium(iv).

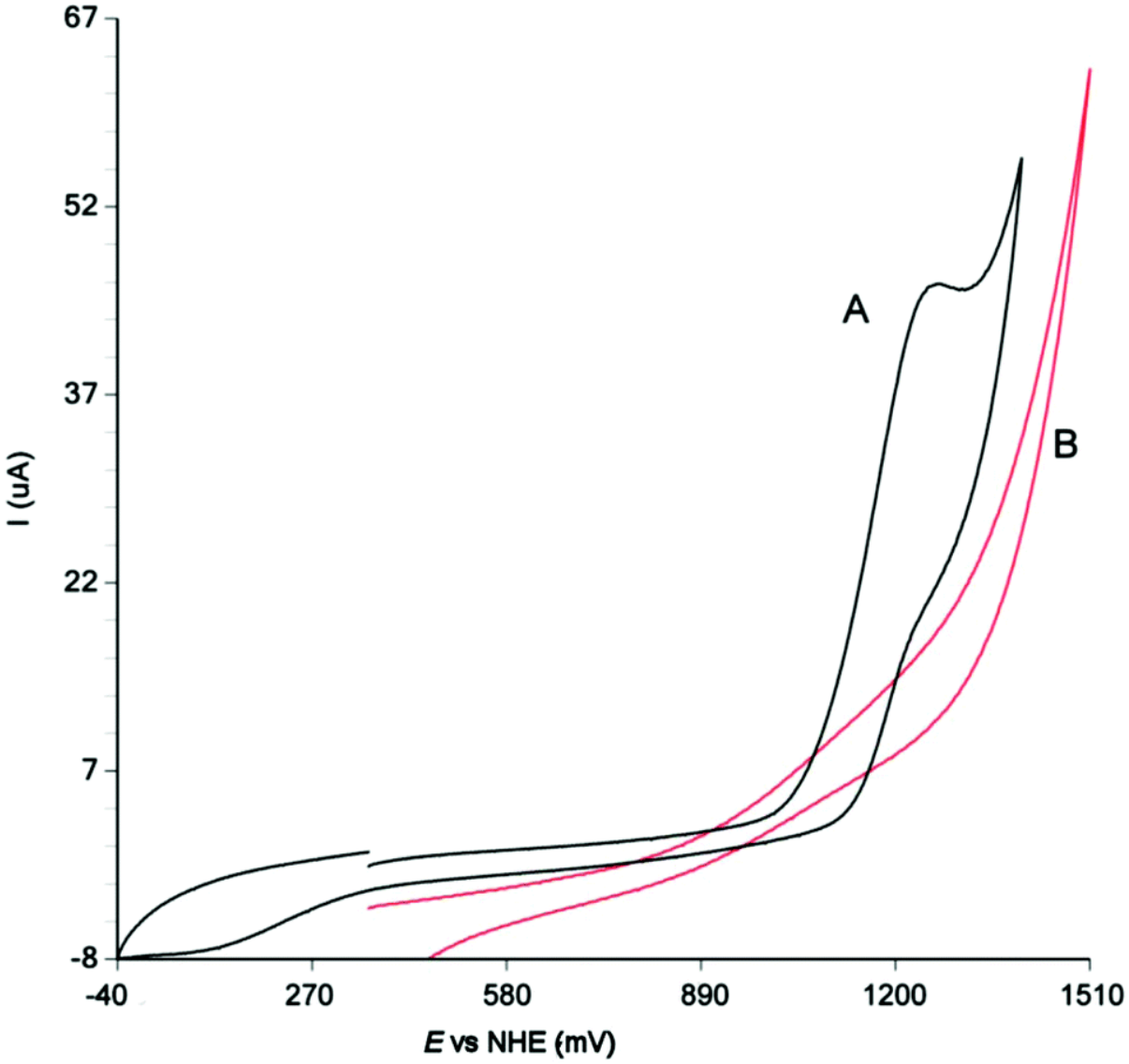

*Figure 5 - Cyclic voltammograms of the complex **1**(A) and the ligand H_3pidiox (B) in methanol. Platinum disk was used as working electrode and platinum wire for both counter and reference electrodes. The supporting electrolyte was tetra-butylammonium perchlorate and the scan rate 100 mV s^{-1}.*

In addition, the CV of **1** in methanol solution gave an irreversible one electron cathodic peak at −153 mV assigned to the reduction of one Ti^{IV} to Ti^{III} {*i.e.* $[Ti^{IV}_6] \rightarrow [Ti^{III}Ti^{IV}_5]$}, and a broad wave at −416 mV assigned to the reduction of the ligand.

UV-vis spectroscopy

The UV-vis spectrum of compound **1** in methanol exhibits two strong absorption bands [(λ/nm, (ε/M^{-1} cm^{-1}): 300 (60 300), 383 (22 400)]. The band at 300 nm was assigned to intraligand π–π*, n–π* and LMCT transition from the ligand to the Ti^{IV} metal ions. This assignment was supported by the UV-vis spectra of the mononuclear metal-H_3pidiox complexes, which exhibit strong absorption at similar wavelengths.[32,34] The broad intense peak at 383 nm was assigned to O–Ti^{IV} LMCT transitions.

NMR spectroscopy

The ^{1}H and ^{13}C NMR chemical shifts of the CD_3OD and D_2O solutions of the ligand H_3pidiox and the complex **1**are depicted in Table 1. The ^{1}H NMR spectrum of the ligand in CD_3OD gave a quintet and a triplet at 1.91 and 2.57 ppm assigned to the two protons attached to C_3 and the four protons attached to C_2 and C_4 respectively; while its ^{13}C NMR spectrum in CD_3OD gave three peaks at 19.32 (C_3), 26.20 (C_2, C_4) and 148.57 (C_1, C_5). The numbering of the carbon and hydrogen atoms of the ligand H_3pidiox is depicted in Scheme 3.

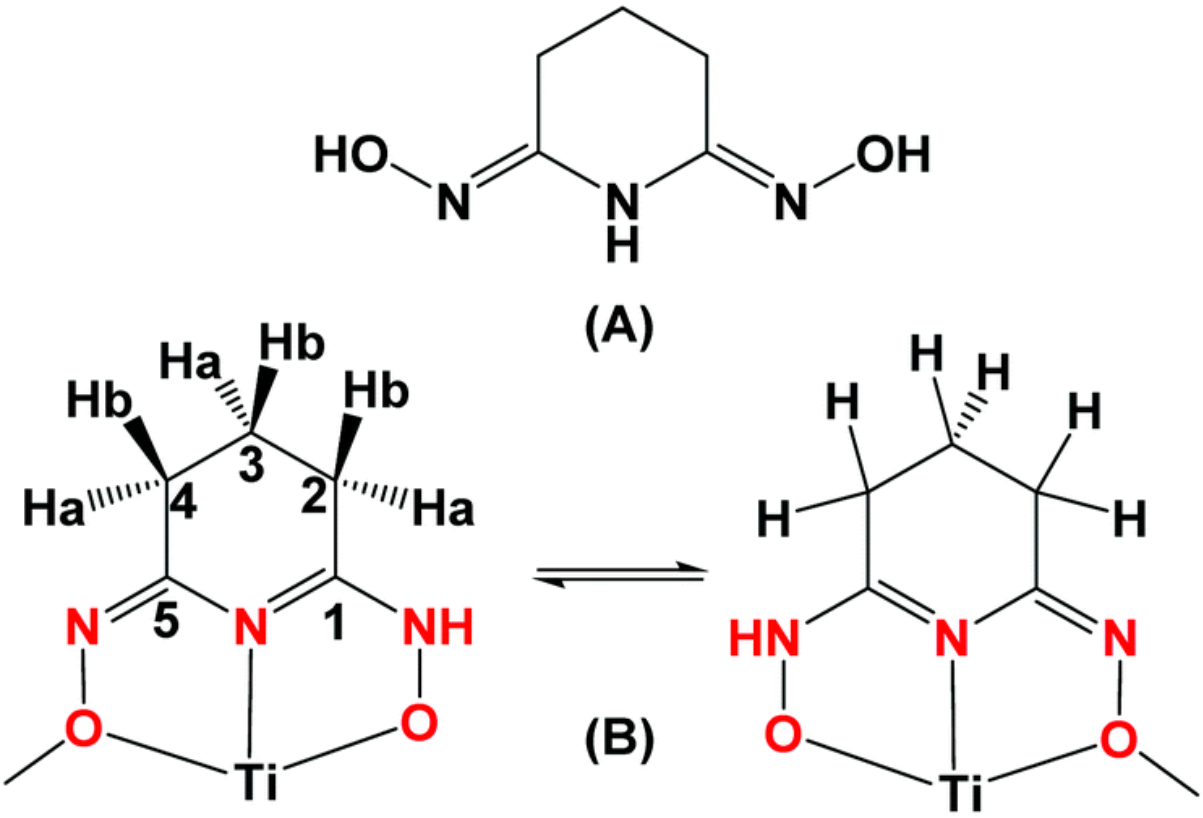

Scheme 3 - The free ligand (A) and the numbering of the carbon and hydrogen atoms of the ligand Hpidiox^{2-} attached to titanium, and the exchange process (B).

*Table 1 - $^{1}H^{a}$ and ^{13}C chemical shifts (ppm) of the complex **1** and the ligand H_3pidiox*

	1[b]		**1**[c]		**H_3pidiox**[b]	
	^{13}C	**^{1}H**	**^{13}C**	**^{1}H**	**^{13}C**	**^{1}H**
C2(Ha)	20.90	2.9284	20.73	2.707	26.20	2.5698
C2(Hb)		2.9284		2.707		2.5698
C3(Ha)	18.17	2.0974	18.07	1.9833	19.31	1.9068

	1[b]		**1**[c]		**H$_3$pidiox**[b]	
	^{13}C	**^{1}H**	**^{13}C**	**^{1}H**	**^{13}C**	**^{1}H**
C3(Hb)		2.3102		2.0873		1.9068
C4(Ha)	20.72	2.8056	20.73	2.652	26.20	2.5698
C4(Hb)		3.0926		2.707		2.5698
C1, C5					148.57	

a The chemical shifts of the protons are the center of multiplets. b In CD_3OD. c In D_2O.

The NMR spectra of the methanol solution **1** show that all ligands attached to titanium(iv) atoms in solution are indistinguishable.

The ^{13}C NMR peaks [found from 2D {^{1}H,^{13}C} grHSQC spectrum, Fig. 6] of the methanol solution of **1** show a shift to higher field in comparison to the free ligand, 18.17 (C_3), 20.72 (C_4) and 20.90 (C_2). It is interesting to note that the C_2 and C_4 carbon atoms are chemically inequivalent in contrast to the free ligand (Scheme 3). This is in agreement with the crystal structure of the complex **1** in which the ligand μ_2-Hpidiox^{2-} is attached to titanium atoms in an asymmetric form (Scheme 3), supporting that the complex retains its structural integrity in solution.

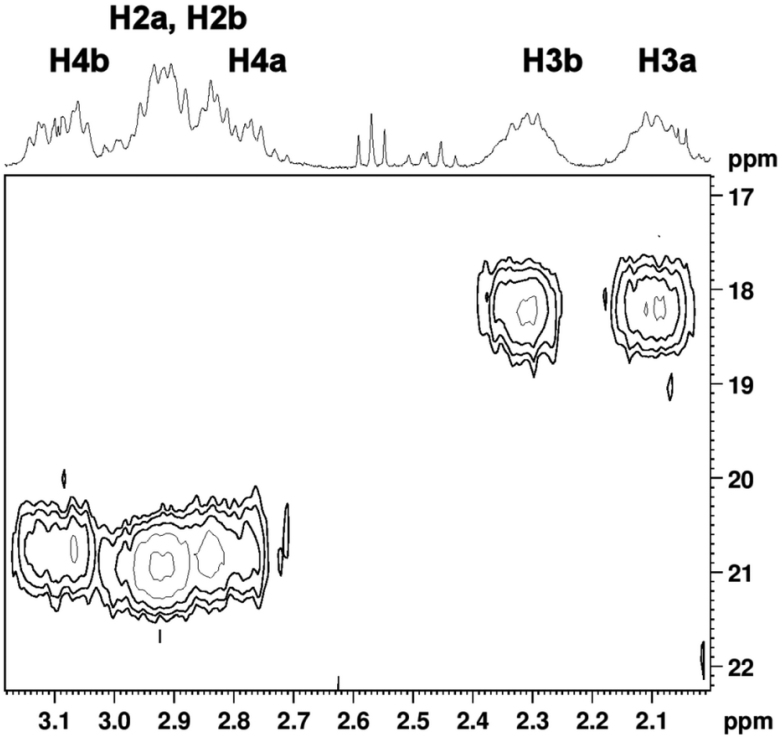

*Figure 6 - The 2D {^{1}H, ^{13}C} grHSQC spectrum of complex **1** in CD_3OD.*

In the ^{1}H NMR spectrum of **1** in CD_3OD the geminal protons of the ligand in each carbon are different and gave different chemical shifts. The^{1}H NMR signals of **1** were assigned using 2D {^{1}H} grCOSY (Fig. S1†), 2D {^{1}H,^{13}C} grHSQC (Fig. 6), and 2D {^{1}H} NOESY (Fig. S2†) spectroscopies. All the hydrogen atoms of the ligands in complex **1**, are correlated with each other in 2D {^{1}H} grCOSY and 2D {^{1}H} grTOCSY spectra suggesting that the six oximes of the complex **1** are equivalent. The H2a and H2b protons' peaks have a δ*v* value (δ*v* = chemical shift difference) approximately equal to the coupling constant (*J*) and thus, gave a second order multiplet centered at 2.928 ppm. The H3a and H3b protons multiplet gave peaks at 2.097 and 2.310 ppm respectively (δ*v* = 0.213 ppm). The δ*v* value between H4a (2.806 ppm) and H4b (3.093 ppm) is 0.287 ppm. The larger δ*v* value of the H4a/H4b protons in comparison with the δ*v* value of H2a/H2b protons, was attributed to the anisotropy induced by the –C=N–O^- oxime double bond next to the H4 protons. Moreover, the 2D {^{1}H} NOESY spectrum of **1** in methanol solution, except to the NOESY cross peaks, gave also EXSY peaks between the H4 and H2 protons and this fact was attributed to the exchange process shown in Scheme 3. The ^{1}H NMR, 2D {^{1}H} grCOSY and 2D {^{1}H,^{13}C} grHSQC spectra of **1** in D_2O gave similar features to those observed in CD_3OD and this supports the fact that **1**retains its structural integrity in aqueous solution (Fig. S3†).

ESI-MS spectrometry

In an effort to characterize further the hexanuclear cluster we employed high resolution ESI-MS to determine unambiguously the structural integrity and composition[52,53] of the titanium-based species in solution.[59–62] The ESI-MS studies were performed in methanol. The observation of the higher intensity set of distribution envelopes is due to the existence of the hexanuclear moiety, resulting from the variable number of protons, counterions and solvent molecules. Additionally, transition metal clusters are generally susceptible to redox processes under the employed ionization conditions which can occasionally induce partial fragmentation of the species. This type of behavior is quite common in ESI-MS solution studies of compounds.[54] The spontaneous or induced fragmentation is quite common approach employed in order to identify stable building blocks and reveal useful details regarding the formation mechanism of the species.[53] In this case, the region of higher *m*/*z*values is populated by a series of distribution envelopes assigned to −1 charged species and correspond to the {Ti_6} cluster (Fig. 7). In this case two of the coordinating groups have been removed during the ionization process (*e.g.* {$Ti^{III}_6O_5(CH_3O)_4(C_5N_3O_2H_7)_4K_2(H_2O)_3H_5$}$^-$). The change of the oxidation state of the metal centers is due to the ionization and consecutive ion-transfer process of the charged species and has been observed previously in numerous occasions.[55]

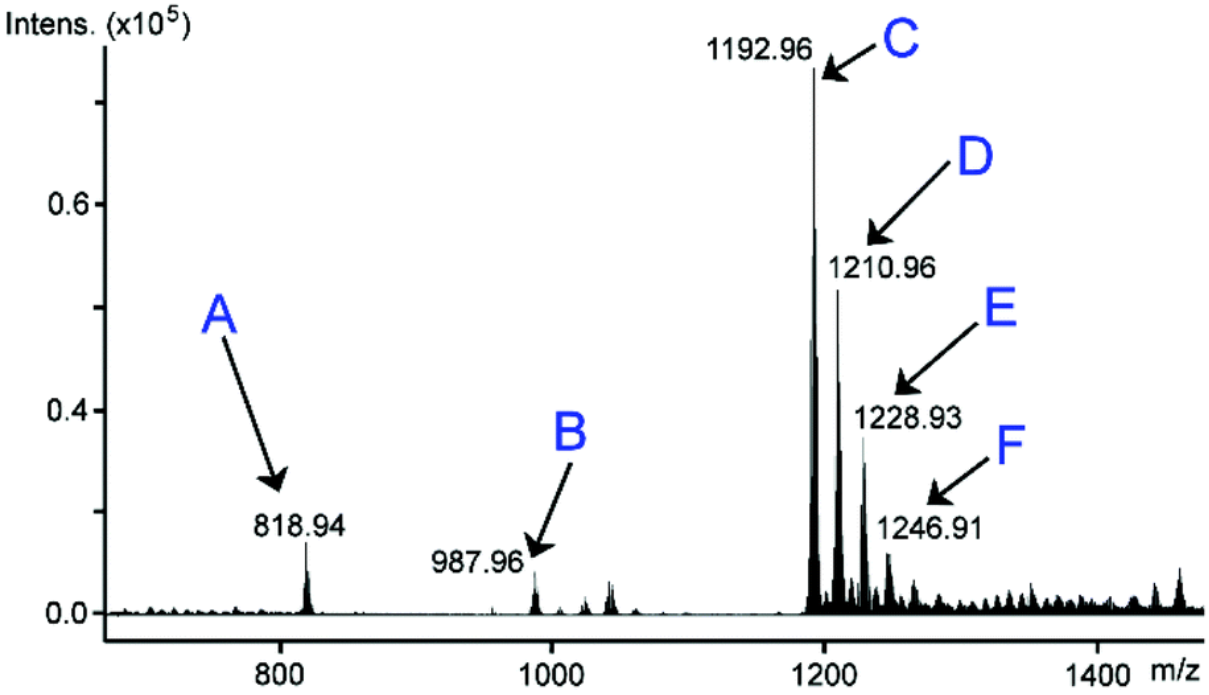

*Figure 7 - Negative ion mass spectrum of **1**; A = $\{Ti^{III}_2Ti^{IV}O(CH_3O)_3(C_5N_3O_2H_7)_3(CH_3OH_2)(H_2O)_6\}^-$, B = $\{Ti^{III}_3O(CH_3O)_3(C_5N_3O_2H_7)_3H_2K_2(CH_3OH_2)_5(H_2O)_4\}^-$, C = $\{Ti^{III}_6O_5(CH_3O)_4(C_5N_3O_2H_7)_4K_2H_5(H_2O)_3\}^-$, D = $\{Ti^{III}_6O_5(CH_3O)_4(C_5N_3O_2H_7)_4K_2H_5(H_2O)_4\}^-$, E = $\{Ti^{III}_6O_5(CH_3O)_4(C_5N_3O_2H_7)_4K_2H_5(H_2O)_5\}^-$, F = $\{Ti^{III}_6O_5(CH_3O)_4(C_5N_3O_2H_7)_4K_2H_5(H_2O)_5\}^-$.*

Interestingly, the lower region of *m/z* values (*ca*. 700–1000) revealed additional information regarding the building block units that have been initially identified by X-ray diffraction analysis, but also showing that the {Ti_6} molecules fragments into their fundamental trimeric building blocks. The distribution envelopes centred at 818.94 and 987.96 *m/z* values have been identified as the intact {Ti_3} units associated with different number of counterions and solvent molecules. The identification of the building blocks that appear in the mass spectrometry studies suggests the existence of an underlying sequential mechanism of assembly, where the initial formation of trimeric clusters[3,4,63] takes place before their subsequently self-assembly into the hexanuclear species that finally crystallize. More specifically, we observed a mixed valence, $\{Ti^{III}_2Ti^{IV}O(CH_3O)_3(C_5N_3O_2H_7)_3H_3(CH_3OH)(H_2O)_6\}^-$ (818.94) and a fully reduced $\{Ti^{III}_3O(CH_3O)_3(C_5N_3O_2H_7)_3H_2K_2(CH_3OH)_5(H_2O)_4\}^-$(987.96) Ti-based oxo centred triangle, respectively.

Theoretical study

Based on the fact that it is not possible to determine the protonation state of the six ligands in cluster **1**, we determined theoretically the relevant stabilities of two Ti^{IV}_6 clusters, one with six H_3pidiox ligands doubly deprotonated {*i.e.*, $[Ti^{IV}_6(Hpidiox)_6]$} and one with four ligands doubly and two fully deprotonated ligands {*i.e.*, $[Ti^{IV}_6(Hpidiox)_4(pidiox)_2]$}. DFT calculations revealed that the cluster $[Ti^{IV}_6(Hpidiox)_4(pidiox)_2]$ with the two $pidiox^{3-}$ligands one on the top of the other [Fig. S4(a)†] is considerably more stable by 14.5 kcal mol^{-1} than $[Ti^{IV}_6(Hpidiox)_6]$ (Fig. S5†). The isomer of the cluster $[Ti^{IV}_6(Hpidiox)_4(pidiox)_2]$ with the two $pidiox^{3-}$ ligands on opposite sides [Fig. S4(b)†] is 4 kcal mol^{-1} less stable than isomer a.

Moreover, in an effort to better understand the redox behaviour observed in **1** we used the hypothetical vanadium(v) complex $[V^V(pidiox)(Hpidiox)]$ as a simpler model [based on the previously

reported vanadium(v) complex[33]]. The plot of spin density of [V^{V}(pidiox)(Hpidiox)] shown in Fig. S6,† reveals that when both ligands pidiox^{3-} and Hpidiox^{2-} coexist in the same complex, the former is susceptible to oxidation.

Metallaromaticity

Formation of trinuclear titanium clusters, instead of the expected mononuclear complex [Ti^{IV}(pidiox)$_2$]$^{2-}$, instigated us to investigate the magnetic diatropic/paratropic (aromatic/antiaromatic)[64] behavior of the *cyclo*-Ti$_3$(μ_2-O)$_3$(μ_3-O) moieties, constituting the **[Ti_6O_5]** oxo-core in **1**. In this context, we used the most popular and quite reliable criterion of the magnetic aromaticity/antiaromaticity, the Nucleus Independent Chemical Shifts (NICS)[65–67] in conjunction with the related NICS$_{zz}$ scan curves.[68] Accordingly, we calculated the NICS$_{zz}$ scan curves for the [*cyclo*-Ti$_3$(μ_2-O)$_3$(μ_3-O)]$_2$ and [*cyclo*-Ti$_3$(μ_2-O)$_3$]$_2$ constituents of the **[Ti_6O_5]** oxo-core employing the GIAO (gauge-including atomic orbitals) DFT method[69,70] as implemented in the Gaussian09 program suite.[71] Calculations were performed using the GIAO/PBE0/6-31G(d,p) computational protocol. The calculated NICS$_{zz}$-curves along with the structures of the model systems used and the 3D plots of the MOs involved in the T$_{x,y}$-allowed HOMO → LUMO transition that mainly contributes to induced diatropic ring current[68,72–78] are shown in Fig. 8.

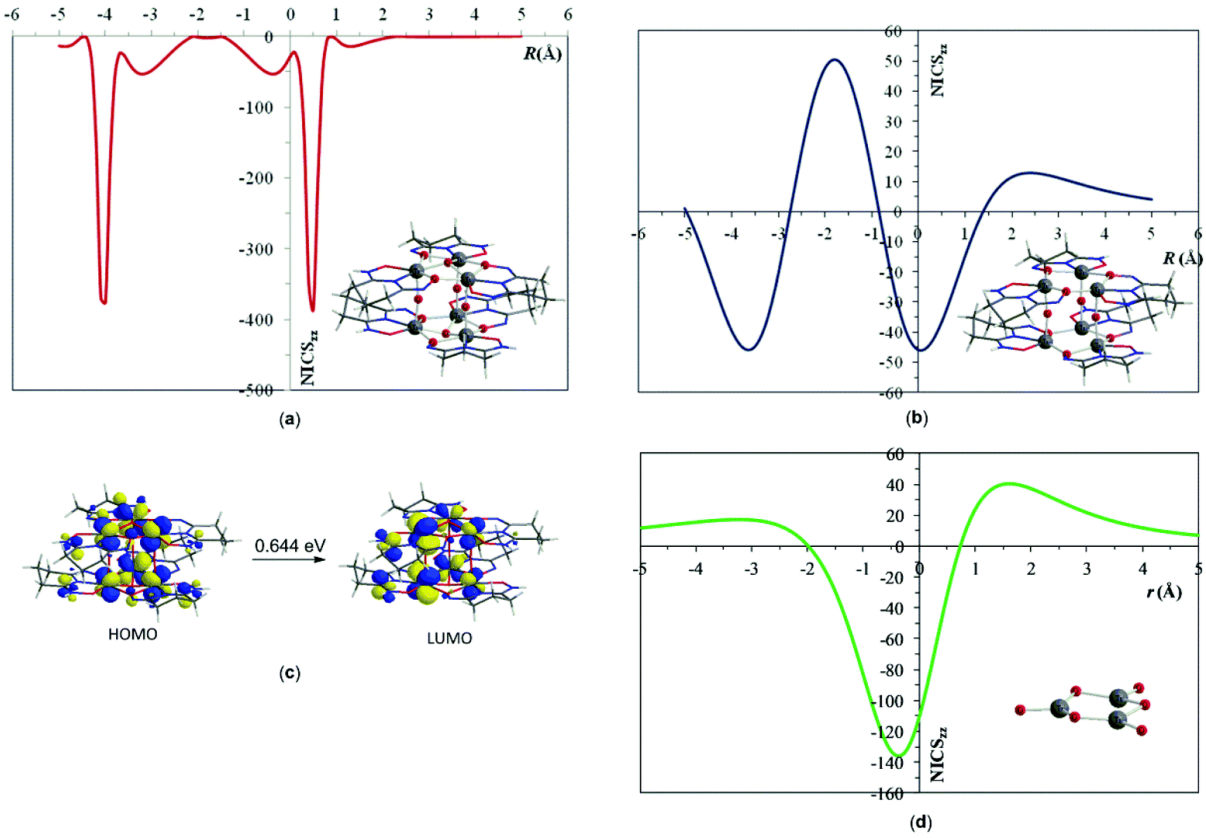

Figure 8 - NICS$_{zz}$ scan curves for the [cyclo-Ti$_3$(μ_2-O)$_3$(μ_3-O)]$_2$ (a) and [cyclo-Ti$_3$(μ_2-O)$_3$]$_2$ (b) constituents of the [Ti_6O_5] oxo-core and the 3D plots of the MOs involved in the T$_{x,y}$-allowed HOMO → LUMO transition (c). NICS$_{zz}$ scan curve for the cyclo-Ti$_3$(μ_2-O)$_3$O$_3$ model system (d).

On the basis of the NICS criterion, it is expected that the capping O atoms do partly reduce aromaticity. An inspection of Fig. 8 reveals that the NICS$_{zz}$ curve calculated for the [*cyclo*-Ti$_3$(μ_2-O)$_3$]$_2$ model system

without the O-capping atom, is more symmetric than that calculated for the [*cyclo*-$Ti_3(\mu\text{-}O)_3(\mu_3\text{-}O)]_2$ model systems.

The $NICS_{zz}$ scan curves of the system without the O capping atoms gave high negative NICS(1) values. Calculations were also performed for a simplified model, *cyclo*-$Ti_3(\mu_2\text{-}O)_3O_3$, including only the trinuclear Ti metallic core, the three terminal and the three bridging O atoms [Fig. 8(d)]. In this system, the three O bridging atoms slightly depart from the plane of the trinuclear Ti core. These three O atoms form also a trinuclear core and the values above 0.7 Å reflect its antiaromatic (paratropic) character. In contrast, the large negative peak indicates that the trinuclear Ti core is highly aromatic.

In the system with O capping atoms there is a multiple superposition of aromatic/antiaromatic zones of the two trinuclear Ti metallic cores along with those of the trinuclear core formed by the three O atoms bridging the two metallic cores. In addition, the O capping atoms probably affect also the aromatic/antiaromatic zones in the opposite to them side, located in the space in between the two metallic cores. Accordingly, the $NICS_{zz}$curve corresponding to the [*cyclo*-$Ti_3(\mu_2\text{-}O)_3(\mu_3\text{-}O)]_2$ model systems exhibits two large peaks around −380 and −390 ppm at 0.5 Å and 4 Å above and below the center of the upper [*cyclo*-$Ti_3(\mu_2\text{-}O)_3(\mu_3\text{-}O)]$ respectively, attributed to the merging of the Bq (Banquo, Bq ghost atoms) into the O capping nuclei. Both of these two sharp peaks are not observed in the $NICS_{zz}$ curve corresponding to the [*cyclo*-$Ti_3(\mu_2\text{-}O)_3]_2$ model system without O capping atoms and obviously arise from the strong contribution to the induced diatropic ring current from the two μ_3-O capping nuclei. The negative $NICS_{zz}(1)$ and $NICS_{zz}(-1)$ values at points 1 Å above and below the center of a molecular ring computed to be −4.3 ppm and −23.2 ppm respectively are indicative for weak aromaticity of the *cyclo*-$Ti_3(\mu_2\text{-}O)_3(\mu_3\text{-}O)$ ring. On the other hand, the negative peak at 1.5 Å with a $NICS_{zz}$ value equal to −12.5 ppm and the $NICS_{zz}(1)$ values for the *cyclo*-$Ti_3(\mu_2\text{-}O)_3$ ring core computed to be around −15 ppm indicate diatropicity of the ring. Interestingly, the computed negative $NICS_{zz}(0)$ values of −45 ppm for the *cyclo*-$Ti_3(\mu_2\text{-}O)_3$ ring illustrates a remarkable in-plane σ-aromaticity of the ring. The main contribution to the diatropic ring current arises from a $T_{x,y}$-allowed HOMO → LUMO excitation amounting to 0.644 eV (Fig. 8c). Both of the magnetically active HOMO and LUMO are composed mainly from 3d AOs of the Ti metal centers, thereby the *cyclo*-$Ti_3(\mu_2\text{-}O)_3$ rings exhibit metallaromaticity, that accounts well for their stability.

Conclusions

In conclusion, following a facile one-pot three-component reaction, a novel hexanuclear oxo-titanium compound **1** with a new structural motif $Ti^{IV}_6O_5$ was synthesized. The cluster is hydrolytically stable in methanol and aqueous solutions suggesting that it can be used further as a building block for the synthesis of larger clusters. $NICS_{zz}$ scan curves, obtained from DFT/GIAO calculation, reveal metallaromaticity for the *cyclo*-Ti_3metallic cores. The rare structural and electronic properties of **1**, suggest that the chemistry described herein can be used for modification of semiconducting materials, such as TiO_2, to new unique materials useful to numerous applications.

Conflicts of interest

There are no conflicts to declare.

References

1 H. Assi, G. Mouchaham, N. Steunou, T. Devic and C. Serre, Chem. Soc. Rev., 2017, 46, 3431–3452.

2 S. Chen, W. H. Fang, L. Zhang and J. Zhang, Inorg. Chem., 2018, 57, 8850–8856.

3 M. Czakler, C. Artner and U. Schubert, New J. Chem., 2018, 42, 12098–12103.

4 M. Czakler and U. Schubert, Inorg. Chim. Acta, 2018, 471, 567–569.

5 W. H. Fang, L. Zhang and J. Zhang, J. Am. Chem. Soc., 2016, 138, 7480–7483.

6 W. H. Fang, L. Zhang and J. Zhang, Chem. Soc. Rev., 2018, 47, 404–421.

7 M. Y. Gao, S. Chen, L. X. Hu, L. Zhang and J. Zhang, Dalton Trans., 2017, 46, 10630–10634.

8 M. Y. Gao, F. Wang, Z. G. Gu, D. X. Zhang, L. Zhang and J. Zhang, J. Am. Chem. Soc., 2016, 138, 2556–2559.

9 J. L. Hou, W. Luo, Y. Guo, P. Zhang, S. Yang, Q. Y. Zhu and J. Dai, Inorg. Chem., 2017, 56, 6451–6458.

10 H. T. Lv, Y. Cui, Y. M. Zhang, H. M. Li, G. D. Zou, R. H. Duan, J. T. Cao, Q. S. Jing and Y. Fan, Dalton Trans., 2017, 46, 12313–12319.

11 H. T. Lv, H. M. Li, G. D. Zou, Y. Cui, Y. Huang and Y. Fan, Dalton Trans., 2018, 47, 8158–8163.

12 G. Zhang, C. Liu, D. L. Long, L. Cronin, C. H. Tung and Y. Wang, J. Am. Chem. Soc., 2016, 138, 11097–11100.

13 S. Yuan, T. F. Liu, D. Feng, J. Tian, K. Wang, J. Qin, Q. Zhang, Y. P. Chen, M. Bosch, L. Zou, S. J. Teat, S. J. Dalgarno and H. C. Zhou, Chem. Sci., 2015, 6, 3926– 3930.

14 J. L. Hou, W. Luo, Y. Y. Wu, H. C. Su, G. L. Zhang, Q. Y. Zhu and J. Dai, Dalton Trans., 2015, 44, 19829–19835.

15 J. X. Yin, P. Huo, S. Wang, J. Wu, Q. Y. Zhu and J. Dai, J. Mater. Chem. C, 2015, 3, 409–415.

16 Y. Y. Wu, P. Wang, Y. H. Wang, J. B. Jiang, G. Q. Bian, Q. Y. Zhu and J. Dai, J. Mater. Chem. A, 2013, 1, 9862– 9868.

17 Z. Liu, J. Lei, M. Frasconi, X. Li, D. Cao, Z. Zhu, S. T. Schneebeli, G. C. Schatz and J. F. Stoddart, Angew. Chem., Int. Ed., 2014, 53, 9193–9197.

18 F. Stehlin, F. Wieder, A. Spangenberg, J. M. Le Meins and O. Soppera, J. Mater. Chem. C, 2014, 2, 277–285.

19 U. Schubert, Coord. Chem. Rev., 2017, 350, 61–67.

20 B. J. Brennan, J. Chen, B. Rudshteyn, S. Chaudhuri, B. Q. Mercado, V. S. Batista, R. H. Crabtree and G. W. Brudvig, Chem. Commun., 2016, 52, 2972–2975.

21 J. L. Hou, P. Huo, Z. Z. Tang, L. N. Cui, Q. Y. Zhu and J. Dai, Inorg. Chem., 2018, 57, 7420–7427.

22 S. Yang, H. C. Su, J. L. Hou, W. Luo, D. H. Zou, Q. Y. Zhu and J. Dai, Dalton Trans., 2017, 46, 9639–9645.

23 Y. Guo, J. L. Hou, W. Luo, Z. Q. Li, D. H. Zou, Q. Y. Zhu and J. Dai, J. Mater. Chem. A, 2017, 5, 18270–18275.

24 H. C. Su, Y. Y. Wu, J. L. Hou, G. L. Zhang, Q. Y. Zhu and J. Dai, Chem. Commun., 2016, 52, 4072–4075.

25 J. F. Wang, W. H. Fang, D. S. Li, L. Zhang and J. Zhang, Inorg. Chem., 2017, 56, 2367–2370.

26 J. D. Sokolow, E. Trzop, Y. Chen, J. Tang, L. J. Allen, R. H. Crabtree, J. B. Benedict and P. Coppens, J. Am. Chem. Soc., 2012, 134, 11695–11700.

27 N. Li, P. D. Matthews, H. K. Luo and D. S. Wright, Chem. Commun., 2016, 52, 11180–11190.

28 C. Chaumont, P. Mobian and M. Henry, Dalton Trans., 2014, 43, 3416–3419.

29 Z. Jiang, J. Liu, M. Gao, X. Fan, L. Zhang and J. Zhang, Adv. Mater., 2016, 28, 1–5.

30 N. Narayanam, W. H. Fang, K. Chintakrinda, L. Zhang and J. Zhang, Chem. Commun., 2017, 53, 8078–8080.

31 G. Tian, S. J. Teat, Z. Zhang and L. Rao, Dalton Trans., 2012, 41, 11579–11586.

32 X. Sun, C. Xu, G. Tian and L. Rao, Dalton Trans., 2013, 42, 14621–14627.

33 C. J. Leggett, B. F. Parker, S. J. Teat, Z. Zhang, P. D. Dau, W. W. Lukens, S. M. Peterson, A. J. P. Cardenas, M. G. Warner, J. K. Gibson, J. Arnold and L. Rao, Chem. Sci., 2016, 7, 2775–2786.

34 D. Sanna, V. Ugone, G. Sciortino, B. F. Parker, Z. Zhang, C. J. Leggett, J. Arnold, L. Rao and E. Garribba, Eur. J. Inorg. Chem., 2018, -, 1805–1816.

35 S. O. Kang, S. Vukovic, R. Custelcean and B. P. Hay, Ind. Eng. Chem. Res., 2012, 51, 6619–6624.

36 N. Singh and S. Bhattacharya, Dalton Trans., 2011, 40, 2707–2710.

37 P. Piszczek, A. Radtke, T. Muzioł, M. Richert and J. Chojnacki, Dalton Trans., 2012, 41, 8261–8269.

38 J. L. Fenton, A. Laaroussi, P. Mobian, C. Chaumont, G. Khalil, C. Huguenard and M. Henry, Eur. J. Inorg. Chem., 2014, -, 357–363.

39 Y. Fan, Y. Cui, G. D. Zou, R. H. Duan, X. Zhang, Y. X. Dong, H. T. Lv, J. T. Cao and Q. S. Jing, Dalton Trans., 2017, 46, 8057–8064.

40 A. Radtke, P. Piszczek, T. Muzioł and A. Wojtczak, Inorg. Chem., 2014, 53, 10803–10810.

41 W. H. Fang, L. Zhang and J. Zhang, Dalton Trans., 2017, 46, 803–807.

42 G. A. Seisenbaeva, E. Ilina, S. Håkansson and V. G. Kessler, J. Sol-Gel Sci. Technol., 2010, 55, 1–8.

43 J. B. Benedict and P. Coppens, J. Am. Chem. Soc., 2010, 132, 2938–2944.

44 K. Hong, W. Bak and H. Chun, Inorg. Chem., 2014, 53, 7288–7293.

45 S. Kim, D. Sarkar, Y. Kim, M. H. Park, M. Yoon, Y. Kim and M. Kim, J. Ind. Eng. Chem., 2017, 53, 171–176.

46 M. Czakler, C. Artner and U. Schubert, Eur. J. Inorg. Chem., 2012, 3485–3489.

47 T. J. Boyle, R. P. Tyner, T. M. Alam, B. L. Scott, J. W. Ziller and B. G. Potter Jr., J. Am. Chem. Soc., 1999, 121, 12104– 12112.

48 X. Fan, N. Narayanam, M. Gao, L. Zhang and J. Zhang, Dalton Trans., 2017, 47, 663–665.

49 C. Wang, C. Liu, X. He and Z. M. Sun, Chem. Commun., 2017, 53, 11670–11673.

50 Y. Y. Wu, W. Luo, Y. H. Wang, Y. Y. Pu, X. Zhang, L. S. You, Q. Y. Zhu and J. Dai, Inorg. Chem., 2012, 51, 8982–8988.

51 A. Pérez-Redondo and A. Martín, Acta Crystallogr., Sect. E: Crystallogr. Commun., 2015, 71, m97.

52 J. X. Liu, M. Y. Gao, W. H. Fang, L. Zhang and J. Zhang, Angew. Chem., Int. Ed., 2016, 55, 5160–5165.

53 N. Narayanam, K. Chintakrinda, W. H. Fang, Y. Kang, L. Zhang and J. Zhang, Inorg. Chem., 2016, 55, 10294– 10301.

54 W. H. Fang, J. F. Wang, L. Zhang and J. Zhang, Chem. Mater., 2017, 29, 2681–2684.

55 L. Ni, D. Liang, Y. Cai, G. Diao and Z. Zhou, Dalton Trans., 2016, 45, 7581–7588.

56 S. Aguado-Ullate, J. J. Carbó, O. González-Del Moral, M. Gómez-Pantoja, A. Hernán-Gómez, A. Martín, M. Mena, J. M. Poblet and C. Santamaría, J. Organomet. Chem., 2011, 696, 4011–4017.

57 S. O. Baumann, M. Bendova, M. Puchberger and U. Schubert, Eur. J. Inorg. Chem., 2011, 573–580.

58 S. O. Baumann, M. Bendova, H. Fric, M. Puchberger, C. Visinescu and U. Schubert, Eur. J. Inorg. Chem., 2009, 3333–3340.

59 H. N. Miras, D. Stone, D. L. Long, E. J. L. McInnes, P. Kögerler and L. Cronin, Inorg. Chem., 2011, 50, 8384–8391.

60 E. F. Wilson, H. N. Miras, M. H. Rosnes and L. Cronin, Angew. Chem., Int. Ed., 2011, 50, 3720–3724.

61 H. Zang, A. Surman, D. Long, L. Cronin and H. N. Miras, Chem. Commun., 2016, 52, 9109–9112.

62 H. Y. Zang, J. J. Chen, D. L. Long, L. Cronin and H. N. Miras, Adv. Mater., 2013, 25, 6245–6249.

63 V. W. Day, T. A. Eberspacher, Y. Chen, J. Hao and W. G. Klemperer, Inorg. Chim. Acta, 1995, 229, 391–405.

64 A. C. Tsipis, Coord. Chem. Rev., 2017, 345, 229–262.

65 P. V. R. Schleyer, C. Maerker, A. Dransfeld, H. Jiao and N. J. R. Van Eikema Hommes, J. Am. Chem. Soc., 1996, 118, 6317–6318.

66 P. Von Ragué Schleyer, M. Manoharan, Z. X. Wang, B. Kiran, H. Jiao, R. Puchta and N. J. R. Van Eikema Hommes, Org. Lett., 2001, 3, 2465–2468.

67 Z. Chen, C. S. Wannere, C. Corminboeuf, R. Puchta and P. von Ragué Schleyer, Chem. Rev., 2005, 105, 3842–3888.

68 A. C. Tsipis, I. G. Depastas and C. A. Tsipis, Symmetry, 2010, 2, 284–319.

69 R. Ditchfield, Mol. Phys., 1974, 27, 789–807.

70 J. Gauss, J. Chem. Phys., 1993, 99, 3629–3643.

71 M. J. Frisch, G. W. Trucks, H. B. Schlegel, G. E. Scuseria, M. A. Robb, J. R. Cheeseman, G. Scalmani, V. Barone, B. Mennucci, G. A. Petersson, et al., Gaussian 09, Revision C.01, 2009.

72 P. Lazzeretti, M. Malagoli and R. Zanasi, Chem. Phys. Lett., 1994, 220, 299.

73 S. Coriani, P. Lazzeretti, M. Malagoli and R. Zanasi, Theor. Chim. Acta, 1994, 89, 181.

74 P. Lazzeretti, in Progress in Nuclear Magnetic Resonance Spectroscopy, ed. J. W. Emsley, J. Feeney and L. H. Sutcliffe, Elsevier, Amsterdam, The Netherlands, 2000, vol. 36, p. 1.

75 E. Steiner and P. W. Fowler, Chem. Commun., 2001, 2220.

76 E. Steiner and P. W. Fowler, J. Phys. Chem. A, 2001, 105, 9553.

77 P. W. Fowler, E. Steiner, R. W. A. Havenith and L. W. Jenneskens, Magn. Reson. Chem., 2004, 42, S68.

78 C. Corminboeuf, R. B. King and P. v. R. Schleyer, ChemPhysChem, 2007, 8, 391.